Novel half-magnetization plateau and nematiclike transition in the $S = 1$ skew chain $Ni_2V_2O_7$

Z. W. Ouyang,[1] Y. C. Sun,[1] J. F. Wang,[1,*] X. Y. Yue,[1] R. Chen,[1] Z. X. Wang,[1]
Z. Z. He,[2,†] Z. C. Xia,[1] Y. Liu,[3] and G. H. Rao[4]

[1]*Wuhan National High Magnetic Field Center & School of Physics, Huazhong University of Science and Technology, Wuhan 430074, People's Republic of China*

[2]*State Key Laboratory of Structural Chemistry, Fujian Institute of Research on the Structure of Matter, Chinese Academy of Sciences, Fuzhou 350002, People's Republic of China*

[3]*School of Physics and Technology, Wuhan University, Wuhan 430072, People's Republic of China*

[4]*School of Materials Science and Engineering, Guilin University of Electronic Technology, Guilin 541004, People's Republic of China*

(Received 19 December 2017; revised manuscript received 26 March 2018; published 11 April 2018)

A quantized magnetization plateau is usually not expected when a classic spin-flop transition occurs in a low-dimensional antiferromagnet. Here, we report an experimental observation of a spin-flop transition followed by a wide half-magnetization plateau in the $S = 1$ skew-chain system $Ni_2V_2O_7$. This plateau, which is stabilized in fields of 8–30 T, is realized through an exotic nematiclike phase transition for magnetic fields applied along all three crystallographic axes, resulting in rich anisotropic phase diagrams. We discuss a possible mechanism whereby the magnetic frustration and interchain interactions may cause this half-magnetization plateau, which is in agreement with our exact diagonalization result.

DOI: 10.1103/PhysRevB.97.144406

I. INTRODUCTION

Quantum magnetization plateaus, in which the magnetization is field independent in a finite field range and its value is a fraction of saturation magnetization [1], are particularly fascinating. For instance, a 1/3 magnetization plateau can be observed in both classical and quantum magnets with the spin number S varying from 1/2 to 5/2. The representative examples include the kagome lattice $Cu_3V_2O_7(OH)_2 \cdot 2H_2O$ [2] and triangular lattices such as Cs_2CuBr_4 [3], $CuFeO_2$ [4], $RbFe(MoO_4)_2$ [5], and $Ba_3CoSb_2O_9$ [6]. A 1/2 magnetization plateau can occur in spin dimers [7], spinels [8], and pyrochlore lattices [9] with strong geometrical frustration and spin-lattice coupling.

For chainlike antiferromagnetic (AFM) systems, the ground state generally corresponds to Néel-type ordering due to interchain coupling so that a quantum magnetization plateau is not expected. For instance, in $Cu_2A_2O_7$ (A = P, As, V), sizable interchain coupling leads to differences in the microscopic magnetic model and enforces long-range AFM ordering, which is associated with long-range superexchange [10]. However, a magnetization plateau of pure quantum origin was indeed observed and typical examples are the 1/3 plateau in the frustrated diamond chain $Cu_3(CO_3)_2(OH)_2$ [11] and the 1/2 plateau in Ni ($S = 1$) bond-alternating chains [12]. In the famous Ising chain $Ca_3Co_2O_6$, a 1/3 plateau appears and it is associated with frustrated interchain AFM exchanges [13]. Note that weakly coupled frustrated zigzag spin chains or spin ladders can produce fractional magnetization plateaus [14–16]. Obviously, the role of geometrical frustration and interchain coupling is essential for the magnetization plateau.

$S = 1$ quantum spin systems are also very interesting because of exotic states. In addition to a 1/2 magnetization plateau in the bond-alternating chains [12] and a 1/3 plateau in the triangular lattice $Ba_3NiAb_2O_9$ (A = Sb, Nb) [17–19], the field dependence of magnetic ordering [20] and an amazing quantum 1/2 plateau were also reported in the $S = 1$ kagome lattice $Ni_3V_2O_8$ [21]. This 1/2 plateau is not expected for kagome lattices based on the necessary condition for a magnetization plateau [1], $n(S - m) =$ integer, where n is the magnetic periodicity and m the height of the plateau. The multisteps in $Ni_3V_2O_8$ as well as the devil's staircase in $S = 1/2$ dimers [22,23] show the elusiveness of the plateau.

Here, we demonstrate a wide 1/2 magnetization plateau and a nematiclike phase in the $S = 1$ skew chain $Ni_2V_2O_7$, which was not seen previously. The $Ni_2V_2O_7$ compound crystallizes in a monoclinic structure with space group $P2_1/c$ [24]. Two types of edge-sharing octahedra, Ni_1O_6 and Ni_2O_6, form bond-alternating skew chains along the c axis [Figs. 1(a) and 1(b)]. Corner-shared nonmagnetic tetrahedrons VO_4 between the skew chains make the compound have a quasi-one-dimensional (1D) structure. He *et al.* [25] synthesized single crystals of $Ni_2V_2O_7$. The magnetization and specific heat data revealed an AFM ordering at $T_N = 7$ K, followed by extra magnetic transitions. However, the $M(T)$ curve does not exhibit a broad peak, as seen in the other Ni spin chain $SrNi_2V_2O_8$ [26], which suggests the disappearance of 1D magnetism in $Ni_2V_2O_7$. This is because in $Ni_2V_2O_7$ there are no Sr^{2+} layers located between the Ni chains, resulting in an enhancement of the interchain interaction and the occurrence of AFM ordering. When the magnetic field is applied along the a axis, a field-induced spin-flop-like transition occurs, and thus $Ni_2V_2O_7$ behaves as a classical three-dimensional (3D) antiferromagnet. The spin-flop transition and large interchain couplings were further supported by electron spin resonance (ESR) and first-principles

*jfwang@hust.edu.cn
†hezz@fjirsm.ac.cn

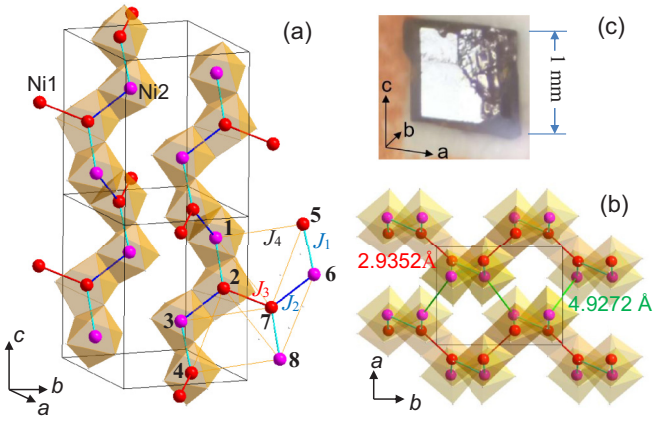

FIG. 1. (a) Coupled skew chain with alternating Ni_1O_6 (red) and Ni_2O_6 (megenta) octahedra along the c axis. (b) A view of the structure along the c axis. In the coupled skew chain, the bond lengths and Ni-O-Ni bond angles: J_1 − 3.0095 Å (95.313° and 95.253°); J_2 − 3.0493 Å (95.567° and 94.411°); and J_3 − 2.9352 Å (98.696°). The J_4 represents the next-nearest-neighboring intrachain and interchain exchanges, which are weak and assumed to be identical due to a small difference in the bond length ranging from 5.0768 to 5.1978 Å. (c) A crystal with a size of 1 mm × 1 mm × 0.3 mm and $\beta = 99.67°$ between the a and c axes.

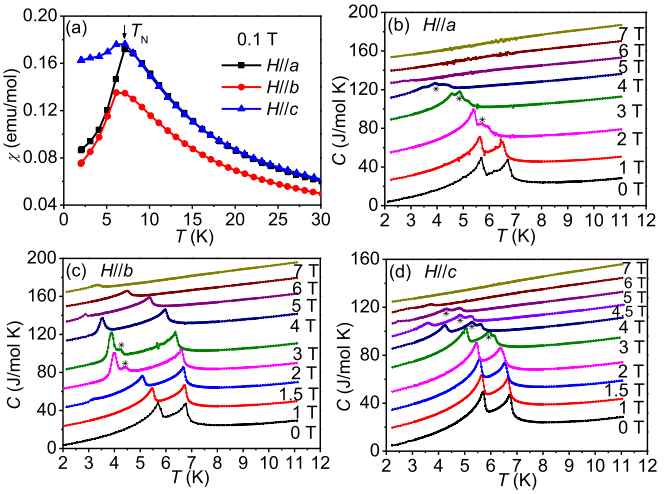

FIG. 2. (a) $\chi(T)$ curves measured at 0.1 T. (b)–(d) Specific heat curves of a single crystal measured at different fields. Extra transitions are marked by stars (*). In relation to the zero-field curve, the curves for 1–7 T are shifted up by various magnitudes: 22, 50, 83, 105, 120, 135, and 150 J/mol K for $H \parallel a$; 20, 40, 60, 80, 110, 130, 145, and 160 J/mol K for $H \parallel b$; and 15, 30, 45, 65, 80, 90, 100, 110, and 120 J/mol K for $H \parallel c$.

studies [27]. With significant interchain coupling and some geometrical frustration ($f = |\theta_p|/T_N = 4$; $\theta_p \sim -25$ K) [25], $Ni_2V_2O_7$ provides a good platform to study the possible quantum phenomenon in an $S = 1$ antiferromagnet with significant interchain coupling. As a result, a 1/2 plateau and a nematiclike phase are observed, in addition to the spin-flop transition.

II. EXPERIMENTAL DETAILS

Single crystals of $Ni_2V_2O_7$ were grown at Fujian Institute of Research on the Structure of Matter, Chinese Academy of Sciences, China. Details of the characterization of the structure and crystallographic axes can be found in Ref. [25]. As shown in Fig. 1(c), the typical size of the crystal is 1 mm × 1 mm × 0.3 mm with $\beta = 99.67°$ between the cleavage directions a and c. Details on the preparation of powder samples can be found in Ref. [27]. Magnetization and specific heat were measured using a commercial physical property measurement system (16-T PPMS). Before each magnetization measurement, the sample was zero-field cooled from the paramagnetic state at 300 K to the desired temperature. Pulsed-high-field magnetization was detected by a standard inductive method employing a couple of coaxial pickup coils. A pulsed magnetic field up to 55 T with a duration time of 24 ms was generated by using a long-pulse magnet energized by two 0.8-MJ capacitor banks, which are installed at Wuhan National High Magnetic Field Center, China.

III. RESULTS AND DISCUSSION

Figure 2(a) displays the temperature dependence of magnetic susceptibility $\chi(T)$ measured at 0.1 T. A cusp characterizing AFM ordering is clearly manifested at $T_N \sim 7$ K when the magnetic field is applied along the a ($H \parallel a$) and b axes ($H \parallel b$), indicating that the a and b directions are the easy magnetization directions. For $H \parallel c$, a slight decrease in magnetization occurs below T_N because the c axis is the hard axis. Note that only an easy a axis was revealed in the previous report [25]. Our recent high-field ESR data demonstrated AFM resonance with uniaxial anisotropy [27].

Specific heat was measured in different fields. As shown in Figs. 2(b)–2(d), the zero-field curve presents two λ-like peaks at 5.7 and 6.7 K. The data are basically in line with an earlier report [25], where the specific heat curve presents two strong peaks at 4.7 and 5.8 K. The small difference in transition temperature is probably because of the difference in data quality. In Ref. [25], the curve does not present good λ-like peaks. An extra weak peak at 8.8 K [25] was not seen along all three axes and thus it may be not intrinsic. The observation of multiple magnetic transitions at low temperatures implies the presence of competing magnetic interactions. As expected for a classical antiferromagnet, both peaks move towards a lower field with an increase of the field. An extra peak marked by stars appears at some fields. Above 7 T, all the peaks are wiped out, signaling the disappearance of AFM ordering and the emergence of a new spin state in the high field.

The $M(H)$ measurements were conducted at 2 K on single crystals with the PPMS magnetometer for a better characterization of the field-induced transitions. As shown in Fig. 3(a), the $M(H)$ curves are highly anisotropic. The curve is linear in low fields due to the AFM ground state. A field-induced spin-flop transition is well established at $H_{sf} = 2.7$ T for $H \parallel a$ and at 1.3 T for $H \parallel b$, but not for $H \parallel c$, again showing that a and b are the easy axes. As the magnetic field increases, the magnetization exhibits anomalies at H_{c1} and H_{c2}, and then tends towards "saturation" above $H_{c2} = 5.5$, 8.0, and 7.1 T for the a, b, and c axes, respectively. The magnetization is unchanged above H_{c2} and does not show magnetic anisotropy.

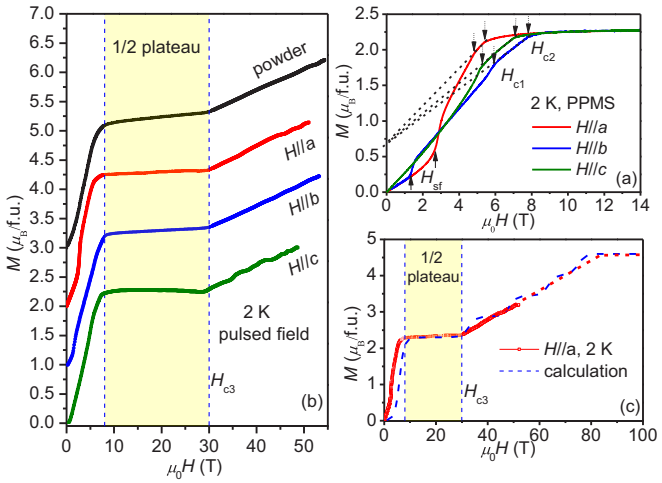

FIG. 3. (a) $M(H)$ curves at 2 K measured with PPMS. The dashed lines are an extrapolation of the linear part between H_{c1} and H_{c2}. (b) High-field $M(H)$ curves at 2 K calibrated with PPMS data. For clarity, the curves for $H \parallel b$, $H \parallel a$, and the powder sample are shifted up by 1.0, 2.0, and 3.0 μ_B/f.u., respectively, in relation to the curve of $H \parallel c$. (c) The high-field $M(H)$ curve for the easy a axis. The blue dashed line is the calculated curve with $g = 2.2$, $J_1 = -9$ K, $J_2 = -38$ K, $J_3 = -17$ K, $J_3 = -6$ K, and $D = -6$ K.

The "saturation" magnetization is about 2.23 μ_B/f.u., which is one half of the expected saturation value of $M_s = 4.4\,\mu_B$/f.u. with $S = 1$ and $g = 2.2$ [27]. This marks the presence of a 1/2 magnetization plateau.

High-field magnetization was measured to examine the field range of the 1/2 plateau. Figure 3(b) shows the results at 2 K calibrated with the PPMS data. The powder curve, the signal of which is better than the small single crystal at high fields, is also plotted for a comparison. Besides the low-field spin-flop transition, the high-field curve reveals a well-defined 1/2 magnetization plateau, which starts approximately at H_{c2} and ends at $H_{c3} = 30$ T for all three directions. For the single crystal, there is almost no contribution from Van Vleck paramagnetism frequently existing in materials exhibiting magnetization plateaus [6]. Above H_{c3}, the magnetization starts to increase linearly up to 55 T with an identical slope for all curves. Extrapolation of the linear part yields magnetic saturation at $\sim H_s = 86$ T [see Fig. 3(c)], which is beyond our experimental condition.

Based on the classical mean-field theory, a spin-flop transition occurs at H_{sf} when the magnetic field is applied along the AFM easy axis (i.e., a and b axes), giving rise to a jump in magnetization. In the spin-flop state, the spins remain antiparallel but their directions are perpendicular to the magnetic field direction. This reflects the presence of large magnetic anisotropy and an interchain interaction in the a-b plane. In a classical picture, the magnetization process is usually simple. Assuming that the AFM ground state is in an "up-down-up-down" type of spin configuration along the skew chain, on application of an external magnetic field, the 1/2 plateau seems to be a natural consequence of flipping one of the four spins, forming an "up-up-up-down" type of configuration. Above the spin-flop field, the magnetization increases linearly by gradually canting the spins away from collinearity until ferromagnetic (FM) saturation, without additional intermediate processes.

The 1/2 magnetization plateau, in which the magnetization is unchanged within a wide field range of 20 T, is far from being trivial. As shown in Fig. 1, the $Ni_2V_2O_7$ contains skew chains along the c axis, in which two nonequivalent Ni ions ($S = 1$) are alternatively aligned as Ni_1-Ni_2-Ni_1-Ni_2 with bond lengths 3.0493 and 3.0095 Å, respectively, quite resembling an $S = 1$ bond-alternating chain. A quantum 1/2 magnetization plateau is therefore expected [12]. Tonegawa *et al.* [28] calculated the phase diagram for a bond-alternating chain and concluded that 1/2 plateaus could occur if $D/J \geqslant 0$ and $\alpha \neq 1$, where D is the single-ion anisotropy, J the nearest-neighboring interaction, and α the bond-alternating ratio between two exchange constants. However, our exact diagonalization results show that such a simple bond-alternating model with the D term fails to produce a well-defined 1/2 plateau.

As shown in Fig. 1(b), the nearest-neighboring Ni_2-Ni_2 distance is 4.9272 Å (the green bond), while the nearest-neighboring Ni_1-Ni_1 distance is 2.9352 Å (the red bond), which is slightly shorter than the bond length along the chain. The interchain couplings should be comparable to the intrachain interactions. These 3D interchain exchanges lead to AFM ordering below 7 K [25], not favoring the occurrence of a plateau. On the other hand, the coupled skew chains form a network of triangularlike tetramers with two Ni_1 and two Ni_2 ions [see sites (1, 2, 3, 7) and (2, 6, 7, 8) in Fig. 1(a)]. In each tetramer, the four Ni ions are coplanar and the triangle with side lengths of 5.1978, 5.1853, and 5.1930 Å is only slightly distorted, favoring a geometrical frustration. Indeed, experimental $T_N = 6.7$ K is low compared to the Weiss temperature $\theta_p = -25$ K [25], indicating the presence of some geometrical frustration ($f = 4$). With geometrical frustration and quantum fluctuations ($S = 1$), a 1/2 quantum plateau is expected. $Ni_2V_2O_7$ could be viewed as a frustrated spin-chain antiferromagnet. It is the frustration and complicated interchain couplings that stabilize the "up-up-up-down" spin configuration, i.e., the 1/2 plateau.

The Hamiltonian for the coupled skew chain can be generally written as

$$H = -\sum_{i,j} J_{ij} S_i \cdot S_{ij} + \sum_{i=1} \left(D S_{iz}^2 + g \mu_B S_{iz} \cdot H \right), \qquad (1)$$

where J_{ij} is the exchange interaction between two sites (i, j). We consider $N = 8$ sites and four types of different couplings [see Fig. 1(a)]. J_1 and J_2 are the alternating intrachain couplings. J_3 is the nearest-neighbor interchain exchange. J_4 represents the next-nearest-neighbor intrachain exchange and interchain exchange. These exchanges are assumed to be identical [see Fig. 1(a)] due to a small difference in the bond length, which varies from 5.0768 to 5.1978 Å. For $N = 8$, the results of the exact diagnalization of Eq. (1) show that the best parameters to describe the 1/2 plateau are $J_1 = -9$ K, $J_2 = -38$ K, $J_3 = -17$ K, $J_4 = -6$ K, and $D = -6$ K. Figure 3(c) manifests the calculated $M(H)$ curve. The D value is of typical magnitude for a Ni compound [29]. All interactions are AFM and the interchain J_3 is comparable

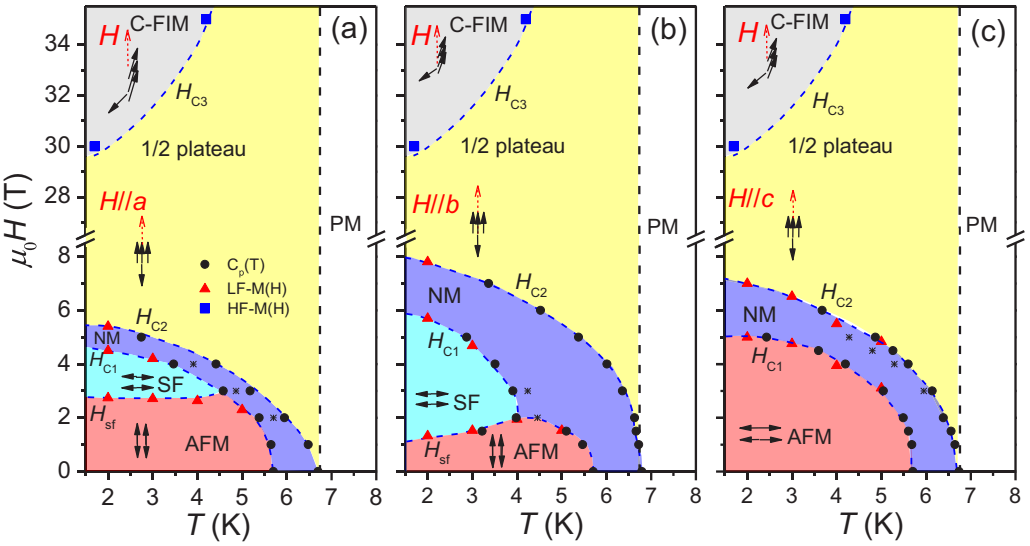

FIG. 4. Field-temperature (H-T) phase diagrams based on the specific heat (●), low-field (LF, ▲), and high-field (HF, ■) $M(H)$ data. The diagram is composed of AFM, spin-flop (SF) AFM, 1/2 plateau, canted ferrimagnetic (C-FIM), and paramagnetic (PM) regions. The blue region between H_{c1} and H_{c2} stands for the nematiclike phase (NM). The isolated data marked by stars (*) stand for extra transitions revealed by the specific data. The arrows show the field direction and spin structures expected at various states.

to the intrachain J_1 and J_2. The averaged value of the dominant exchanges $(2J_1 + J_2 + J_3)/4$ is about -18.4 K, very close to the effective interaction of $J = -18.7$ K derived after the formula $\theta_p = 2S(S+1)J/3$ [30].

Recently [27], from a first-principles study, we obtained the following exchange interactions: $J_1 = -33.5$ K, $J_2 = -37.4$ K, and $J_3 = -470$ K for general gradient approximation (GGA) calculations and $J_1 = -1.8$ K, $J_2 = -6.0$ K, and $J_3 = -161$ K for GGA + U ($U_{\text{eff}} = 4.5$ eV) calculations, respectively. In the calculations, J_4 is ignored for simplicity. Theory indeed predicts a large interchain interaction, in qualitative accordance with the results of high-field magnetization. However, J_3 is too big and the calculated values strongly depend on the U_{eff} term. Thus, the exchange interactions based on the exact diagonalization of Eq. (1) are more reasonable. Note that the difference between J_1 and J_2 is not anticipated because they correspond to similar bond lengths and Ni-O-Ni bond angles. We stress that our Hamiltonian model with eight sites (two J_1, one J_2, and one J_3) is only a simple approximation. Theoretical calculations with more sites could diminish the large J_1-J_2 difference and produce a smooth $M(H)$ curve above H_{c3}, meanwhile wiping out the small spin gap in low fields.

In addition to the 1/2 plateau, the classical mean-field theory cannot capture the linear feature between H_{c1} and H_{c2} in the $M(H)$ curves. As shown in Fig. 3(a), the extrapolation of the linear region to zero field points to the same magnetic moment of $\sim 0.7\,\mu_B$/f.u., namely, $1/3 M_{\text{plateau}}$, independent of the field direction. This might suggest the presence of nonclassical spin nematic ordering, in which bound magnon pairs are condensed in a high magnetic field near the saturation point. This unconventional magnetic phase was theoretically predicted [31,32], but rarely observed in experiments. Recently, the quasi-1D frustrated magnet $LiCuVO_4$ and the distorted kagome antiferromagnet $Cu_3V_2O_7(OH)_2 \cdot 2H_2O$ presented a sign of spin-nematic-like ordering, in which the magnetization varies linearly with magnetic field before the saturation field H_{sat} [2,33]. Especially in $LiCuVO_4$, the $M(H)$ curve along the a and b axes exhibited a spin-flop transition and a strong inflection, followed by a linear region with a slope of $\sim 1/2 M_{\text{sat}}/H_{\text{sat}}$, quite similar to our case of $Ni_2V_2O_7$. The field for the onset of the 1/2 plateau, H_{c2}, could be analogous to a "saturation" field. Thus, the linear $M(H)$ curve between H_{c1} and H_{c2} in $Ni_2V_2O_7$ indeed resembles a macroscopic manifestation of a nematiclike phase [33].

Based on the available magnetization and specific heat data, we plot in Fig. 4 the magnetic field-temperature (H-T) phase diagrams, in which the classical spin-flop transition coexists with the quantum 1/2 magnetization plateau. In zero field, the spins are aligned in the ab plane. Above H_{sf}, the spins become perpendicular to the applied field direction. Between H_{c1} and H_{c2} is the new nematiclike phase. The isolated data marked by stars stand for extra transitions revealed by the specific data, which might be associated with the formation of nematiclike phases. In the quantum 1/2 magnetization plateau, a collinear up-up-up-down configuration is formed and stabilized by frustration and quantum fluctuations. Above H_{c3} is the canted ferrimagnetic (C-FIM) state, where the magnetization starts growing linearly by gradually canting the spins away from collinearity until FM saturation. This $S = 1$ spin system exhibits a spin-flop, magnetization plateau, and nematiclike phase at the same time. As shown in Fig. 4, the complicated anisotropic H-T diagram of $Ni_2V_2O_7$ contains rich physics, especially field-induced exotic phases. Our study is expected to stimulate further theoretical investigations on spin systems with significant interchain couplings.

IV. CONCLUSIONS

In summary, we have studied a novel type of stable magnetization plateau in the low-D spin-chain system $Ni_2V_2O_7$, where the spin-flop transition and accompanying nematiclike

transition cooperatively induce a novel half-magnetization plateau. Considering the interchain interactions and geometric frustration, we propose a model of a triangularlike tetramer with "up-up-up-down" spin arrangements, which is qualitatively consistent with our exact diagonalization result. The study of quantized magnetization plateaus in low-dimensional frustrated magnets has aroused continuous interests in the past decade. We believe that the $Ni_2V_2O_7$ compound is a good candidate material for studying interchain-coupled spin-chain systems and the exotic spin nematic state in quantum magnets.

ACKNOWLEDGMENTS

This work was supported by the National Natural Science Foundation of China (Grants No. 11474110 and No. 11574098). Z.Z.H. is grateful to the Joint Fund of Research Utilizing Large-Scale Scientific Facilities under a cooperative agreement between NSFC and CAS (No. U1632159). Z.C.X. is grateful for support from the National Key Research and Development Program of China (Grant No. 2016YFA0401003) and the Natural Science Foundation of China (Grant No. 11674115).

[1] M. Oshikawa, M. Yamanaka, and I. Affleck, Phys. Rev. Lett. **78**, 1984 (1997).
[2] H. Ishikawa, M. Yoshida, K. Nawa, M. Jeong, S. Krämer, M. Horvatić, C. Berthier, M. Takigawa, M. Akaki, A. Miyake, M. Tokunaga, K. Kindo, J. Yamaura, Y. Okamoto, and Z. Hiroi, Phys. Rev. Lett. **114**, 227202 (2015).
[3] T. Ono, H. Tanaka, H. Aruga Katori, F. Ishikawa, H. Mitamura, and T. Goto, Phys. Rev. B **67**, 104431 (2003).
[4] N. Terada, Y. Narumi, K. Katsumata, T. Yamamoto, U. Staub, K. Kindo, M. Hagiwara, Y. Tanaka, A. Kikkawa, H. Toyokawa, T. Fukui, R. Kanmuri, T. Ishikawa, and H. Kitamura, Phys. Rev. B **74**, 180404 (2006).
[5] L. E. Svistov, A. I. Smirnov, L. A. Prozorova, O. A. Petrenko, L. N. Demianets, and A. Y. Shapiro, Phys. Rev. B **67**, 094434 (2003).
[6] Y. Shirata, H. Tanaka, A. Matsuo, and K. Kindo, Phys. Rev. Lett. **108**, 057205 (2012).
[7] Y. H. Matsuda, N. Abe, S. Takeyama, H. Kageyama, P. Corboz, A. Honecker, S. R. Manmana, G. R. Foltin, K. P. Schmidt, and F. Mila, Phys. Rev. Lett. **111**, 137204 (2013).
[8] A. Miyata, H. Ueda, Y. Ueda, H. Sawabe, and S. Takeyama, Phys. Rev. Lett. **107**, 207203 (2011).
[9] Y. Okamoto, D. Nakamura, A. Miyake, S. Takeyama, M. Tokunaga, A. Matsuo, K. Kindo, and Z. Hiroi, Phys. Rev. B **95**, 134438 (2017).
[10] O. Janson, A. A. Tsirlin, J. Sichelschmidt, Y. Skourski, F. Weickert, and H. Rosner, Phys. Rev. B **83**, 094435 (2011).
[11] H. Kikuchi, Y. Fujii, M. Chiba, S. Mitsudo, T. Idehara, T. Tonegawa, K. Okamoto, T. Sakai, T. Kuwai, and H. Ohta, Phys. Rev. Lett. **94**, 227201 (2005).
[12] Y. Narumi, K. Kindo, M. Hagiwara, H. Nakano, A. Kawaguchi, K. Okunishi, and M. Kohno, Phys. Rev. B **69**, 174405 (2004).
[13] V. Hardy, M. R. Lees, O. A. Petrenko, D. McK. Paul, D. Flahaut, S. Hébert, and A. Maignan, Phys. Rev. B **70**, 064424 (2004).
[14] A. K. Kolezhuk, Phys. Rev. B **59**, 4181 (1999).
[15] B. Kurniawan, H. Tanaka, K. Takatsu, W. Shiramura, T. Fukuda, H. Nojiri, and M. Motokawa, Phys. Rev. Lett. **82**, 1281 (1999).
[16] T. Sugimoto, M. Mori, T. Tohyama, and S. Maekawa, Phys. Rev. B **92**, 125114 (2015).
[17] Y. Shirata, H. Tanaka, T. Ono, A. Matsuo, K. Kindo, and H. Nakano, J. Phys. Soc. Jpn. **80**, 093702 (2011).
[18] J. Hwang, E. S. Choi, F. Ye, C. R. Dela Cruz, Y. Xin, H. D. Zhou, and P. Schlottmann, Phys. Rev. Lett. **109**, 257205 (2012).
[19] J. Richter, O. Götze, R. Zinke, D. J. J. Farnell, and H. Tanaka, J. Phys. Soc. Jpn. **82**, 015002 (2013).
[20] M. Kenzelmann, A. B. Harris, A. Aharony, O. Entin-Wohlman, T. Yildirim, Q. Huang, S. Park, G. Lawes, C. Broholm, N. Rogado, R. J. Cava, K. H. Kim, G. Jorge, and A. P. Ramirez, Phys. Rev. B **74**, 014429 (2006).
[21] J. F. Wang, M. Tokunaga, Z. Z. He, J. I. Yamaura, A. Matsuo, and K. Kindo, Phys. Rev. B **84**, 220407 (2011).
[22] K. Siemensmeyer, E. Wulf, H. J. Mikeska, K. Flachbart, S. Gabáni, S. Mat'aš, P. Priputen, A. Efdokimova, and N. Shitsevalova, Phys. Rev. Lett. **101**, 177201 (2008).
[23] M. Takigawa, M. Horvatić, T. Waki, S. Krämer, C. Berthier, F. Lévy-Bertrand, I. Sheikin, H. Kageyama, Y. Ueda, and F. Mila, Phys. Rev. Lett. **110**, 067210 (2013).
[24] E. E. Sauerbrei, R. Faggiani, and C. Calvo, Acta Crystallogr. B **30**, 2907 (1974).
[25] Z. He, J. I. Yamaura, Y. Ueda, and W. D. Cheng, Phys. Rev. B **79**, 092404 (2009).
[26] Z. He and Y. Ueda, J. Phys. Soc. Jpn. **77**, 013703 (2008).
[27] Y. C. Sun, Z. W. Ouyang, J. F. Wang, Z. X. Wang, Z. C. Xia, and G. H. Rao, Eur. Phys. J. Plus **131**, 343 (2016).
[28] T. Tonegawa, T. Nakao, and M. Kaburagi, J. Phys. Soc. Jpn. **65**, 3317 (1996).
[29] A. K. Bera, B. Lake, A. T. M. N. Islam, B. Klemke, E. Faulhaber, and J. M. Law, Phys. Rev. B **87**, 224423 (2013).
[30] M. Hase, T. Yang, R. Cong, J. Lin, A. Matsuo, K. Kindo, K. Ozawa, and H. Kitazawa, Phys. Rev. B **80**, 054402 (2009).
[31] T. Hikihara, L. Kecke, T. Momoi, and A. Furusaki, Phys. Rev. B **78**, 144404 (2008).
[32] F. Heidrich-Meisner, I. P. McCulloch, and A. K. Kolezhuk, Phys. Rev. B **80**, 144417 (2009).
[33] N. Büttgen, K. Nawa, T. Fujita, M. Hagiwara, P. Kuhns, A. Prokofiev, A. P. Reyes, L. E. Svistov, K. Yoshimura, and M. Takigawa, Phys. Rev. B **90**, 134401 (2014).